New Physics: Sae Mulli,
Vol. 67, No. 11, November 2017, pp. 1312∼1318
http://dx.doi.org/10.3938/NPSM.67.1312

Analysis of α + ^{16}O Elastic Scattering in the Coulomb-Modified Glauber Model

Yong Joo KIM*
Department of Physics and Research Institute for Basic Sciences, Jeju National University, Jeju 63243, Korea

(Received 8 September 2017 : revised 29 September 2017 : accepted 29 September 2017)

We analyze the elastic scattering of the α + ^{16}O system at 240 and 400 MeV within the framework of the Coulomb-modified Glauber model by using an effective nucleon-nucleon (NN) amplitude considering a q^4 component. The calculated results show a fairly good agreement with the experimental data. The near-side and the far-side decompositions of the elastic cross section have also been performed by following Fuller's formalism. The presence of a nuclear rainbow is evidenced by a classical deflection function. We also investigate the effect of a q^4 component of the effective NN amplitude on the elastic and the reaction cross sections. The effective NN amplitude is found to be helpful in reproducing the α + ^{16}O elastic scattering data.

PACS numbers: 24.10.-i, 25.70.-z, 25.70.Bc
Keywords: Coulomb-modified Glauber model, Effective NN amplitude, In-medium NN total cross section, Elastic scattering, α + ^{16}O

I. INTRODUCTION

A number of efforts [1–10] have been made to study the heavy-ion elastic scattering within the framework of the optical limit approximation (OLA) to the Glauber model. The important ingredient needed for describing the elastic cross section is the nuclear phase shift. In this approximation, only the leading term in an expansion of the nucleus-nucleus phase shift function is considered. The standard form of OLA to the Glauber model was modified [3] to account for the deviation in the straight-line trajectory because of the Coulomb field. This type of OLA to the Glauber model is called as a "Coulomb-modified Glauber model (CMGM)".

The CMGM has been used as simple and useful tool in describing the heavy-ion elastic scattering at high energies. The main components of CMGM are the densities of colliding nuclei and the nucleon-nucleon (NN) scattering amplitude. Due to its simplicity, CMGM has been advanced to study the heavy-ion elastic and reaction cross sections at low and intermediate energies. Charagi [11] has extended the CMGM to low energies by calculating the overlap integral of the nuclear densities over a hyperbolic trajectory. It predicted reasonably well the reaction cross sections of a large number of heavy-ion systems at low energy range. Analysis of 240 MeV α particle elastic scatterings on ^{58}Ni, ^{116}Sn and ^{197}Au has been performed [12] with the effective $N-\alpha$ amplitude in the CMGM. The α+ nucleus elastic data have been studied [13] extensively over a wide energy range by using the CMGM including the higher momentum transfer components of NN amplitude.

In our earlier study [14], we have presented a semiclassical phase shift analysis of the elastic data for E_{lab} = 1503 MeV ^{16}O beams on ^{40}Ca and ^{90}Zr nuclei based on the CMGM. Recently, the ^{6}Li + ^{92,94,96}Zr elastic scatterings at E_{lab} = 70 MeV have been analyzed [15] within the framework of the CMGM by using the effective NN amplitude having the $\lambda_1 q^4 + \lambda_2 q^6$ (q is momentum transfer). The elastic scatterings of α + ^{16}O system have been measured [16,17] up to small (for E_{lab} = 240 MeV) and relatively large angles (for E_{lab} = 400 MeV), and analyzed by using the optical and single folding models, respectively. In this paper, we present a CMGM by

*E-mail: yjkim@jejunu.ac.kr

using the effective NN amplitude (ENNA) considering a q^4 component, and examine its usefulness by analyzing the α + ^{16}O system at E_{lab} = 240 and 400 MeV. Two free parameters (λ_R and λ_I) related with the coefficients of q^4 in ENNA are used to analyze the elastic data because the α_{NN} (ratio of real to imaginary parts of the forward NN scattering amplitude) is determined from the CMGM with the conventional NN amplitude (CNNA). Other elements are the nuclear densities and the NN total cross section. The main concerns in this paper are as follows : (1) $\chi^2/N-$ fit to the elastic scattering cross sections, and necessity of the introduction of the in-medium NN total cross section, (2) the contributions of the near-side and the far-side components to the angular distributions, (3) the deflection function, the modulus of S-matrix element, and the strong absorption radius , and (4) the effect of $\lambda_R q^4$ and $\lambda_I q^4$ on the elastic and reaction cross sections. In the next section, we briefly describe the theory regarding the CMGM by using the ENNA. The numerical results are presented and discussed in Sec. III. Finally, Sec. IV contains the concluding remarks.

II. THEORY

According to the OLA to the Glauber model, the nuclear phase shift $\delta(b)$ in the impact parameter b space may be written as [18,19]

$$\delta(b) = \frac{A_P A_T}{2k_{NN}} \int_0^\infty dq q J_0(qb) f_{NN}(q) F_P(q) F_T(q), \quad (1)$$

where q is the momentum transfer, k_{NN} is the nucleon momentum corresponding to the projectile kinetic energy per nucleon and $J_0(qb)$ is the Bessel function of zeroth order. Both $F_P(q)$ and $F_T(q)$ are the form factors for the projectile (P) and target (T) nuclei, respectively. At the same time, $f_{NN}(q)$ is NN scattering amplitude. By assuming nuclear densities as a Gaussian form

$$\rho_i(r) = \rho_i(0) \exp\left(-\frac{r^2}{a_i^2}\right), \quad i = P, T \quad (2)$$

and using the Fourier transformation of $\rho_i(r)$, we can obtain the nuclear form factor

$$F_i(q) = \exp(-q^2 a_i^2/4), \quad i = P, T \quad (3)$$

where the density parameters $\rho_i(0)$ and a_i with root-mean-square radius R^i_{rms} are given by

$$a_i = \frac{R^i_{rms}}{\sqrt{1.5}}, \quad \rho_i(0) = \frac{1}{(a_i\sqrt{\pi})^3}. \quad (4)$$

Concerning the $f_{NN}(q)$, we take the following effective NN amplitude given by [13]

$$f_{NN}(q) = \frac{k_{NN}}{4\pi}\sigma_{NN}(\alpha_{NN} + i)\exp[-\beta_{NN}q^2/2][1 + \lambda q^4] \quad (5)$$

instead of conventional NN amplitude with $\lambda = 0$. In this equation, α_{NN} is the ratio of real to imaginary parts of the forward NN scattering amplitude, β_{NN} is the slope parameter, and λ is the free parameter. The nucleon-nucleon total cross section σ_{NN} averaged over neutron and proton numbers is calculated by the expression

$$\sigma_{NN} = \frac{N_P N_T \sigma_{nn} + Z_P Z_T \sigma_{pp} + N_P Z_T \sigma_{np} + N_T Z_P \sigma_{np}}{A_P A_T} \quad (6)$$

where σ_{pp} (σ_{nn}) and σ_{np} are obtained from Eqs. (22) and (23) by Charagi and Gupta [4]. When the medium effect on NN total cross sections is taken into account, $\sigma_{nn}(\sigma_{pp})$ and σ_{np} will be replaced by the formula [20]:

$$\sigma^m_{ij} = \sigma_{ij} \times f_m(ij), \qquad i, j = p, n \quad (7)$$

with the in-medium factors $f_m(ii)$ and $f_m(ij)$

$$f_m(ii) = \frac{1 + 7.772E^{0.06}_{lab}\rho^{1.48}}{1 + 18.01\rho^{1.46}}, \qquad i = j \quad (8)$$

and

$$f_m(ij) = \frac{1 + 20.88E^{0.04}_{lab}\rho^{2.02}}{1 + 35.86\rho^{1.90}}, \qquad i \neq j \quad (9)$$

where E_{lab} is the incident nucleon energy in MeV, and ρ is the nuclear matter density in units of fm^{-3}. Inserting Eqs. (3) and (5) into Eq. (1), we can obtain an analytic expression of the nuclear phase shift as

$$\delta(b) = \frac{A_P A_T}{4\pi}\sigma_{NN}(\alpha_{NN} + i) \times \left[\frac{1}{R^2} + \lambda\frac{16}{R^6}(2 + \frac{b^4}{R^4} - \frac{4b^2}{R^2})\right]\exp\left[-\frac{b^2}{R^2}\right] \quad (10)$$

with

$$R^2 = a_P^2 + a_T^2 + 2\beta_{NN}. \quad (11)$$

Table 1. Input parameters and χ^2/N values in the CMGM for the α + ^{16}O elastic scattering at 240 and 400 MeV. We have used $a_P = 1.396\ fm$ and $a_T = 2.213\ fm$ obtained from the root-mean square radius [21]. Set 1 and Set 2 are the input parameters by using the free and the in-medium NN total cross sections, respectively. The χ^2/N values denote the results by using the effective (conventional) NN amplitude.

Energy (MeV)		$\sigma_{NN}(mb)$	α_{NN}	$\beta_{NN}(fm^2)$	$\lambda(fm^4)$	χ^2/N^a
240	Set 1	88.8	1.573	0.5318	-0.010-0.409i	1.42 (3.79)
	Set 2	64.8	1.900	0.5318	-0.087-0.051i	0.92 (1.10)
400	Set 1	51.0	1.005	0.51	-0.273+0.032i	9.32 (14.11)
	Set 2	37.7	1.266	0.51	-0.170+0.064i	6.41 (10.20)

[a] 10 error bars, $\chi^2/N = (1/N)\sum_{i=1}^{N}\left[\frac{\sigma_{\rm th}(\theta_i)-\sigma_{\rm ex}(\theta_i)}{\Delta\sigma_{\rm ex}(\theta_i)}\right]^2$.

In a CMGM, the impact parameter $b = \sqrt{L(L+1)}/k$ is replaced by the distance of closest approach r_c :

$$r_c = \frac{1}{k}(\eta + \sqrt{\eta^2 + L(L+1)}) \tag{12}$$

where η is the Sommerfeld parameter. Then the nuclear phase shift $\delta(b)$ in Eq. (10) can be replaced by an expression $\delta_L(r_c)$ in terms of L.

The elastic scattering amplitude for spin-zero particles via Coulomb and short-range central forces can be written in the form

$$f(\theta) = f_R(\theta) + \frac{1}{ik}\sum_{L=0}^{\infty}(L+\frac{1}{2})\exp(2i\sigma_L)(S_L-1)P_L(\cos\theta), \tag{13}$$

where $f_R(\theta)$ is the usual Rutherford scattering amplitude, σ_L is the Coulomb phase shift, and S_L is the nuclear scattering matrix element given by

$$S_L = \exp[2i\delta_L(r_c)]. \tag{14}$$

III. RESULTS AND DISCUSSION

Following the approach discussed in the previous section, we have calculated the elastic differential cross sections of α + ^{16}O system at E_{lab} = 240 and 400 MeV by using the ENNA in the CMGM. The inputs required for calculation are (i) the parameters a_i of the form factors for the colliding nuclei and (ii) the NN amplitude parameters : σ_{NN}, α_{NN}, β_{NN} and λ. The a_i values of Eq. (3) are calculated from Eq. (4), where root-mean-square radii R^i_{rms} are taken from Ref. [21]. The value of the free space NN total cross section (σ^f_{NN}) was obtained by taking $\rho = 0.0\ fm^{-3}$ in the Eqs. (7)-(9). For the calculation of the in-medium NN total cross section (σ^m_{NN}), we used $\rho = 0.19\ fm^{-3}$ [20] in the Eqs. (7)-(9). Regarding the slope parameter, β_{NN} = 0.51 fm^2 at 100 MeV/nucleon is taken from Ref. [21]. In the case of 60 MeV/nucleon, we used β_{NN} = 0.5318 fm^2, which was interpolated from the β_{NN} values at 45 and 100 MeV/nucleon [21]. The calculations of elastic cross section have been performed by using the σ^f_{NN} and the σ^m_{NN}, respectively. Based on the CMGM by using CNNA, we first determined the parameter α_{NN} from fitting the elastic data. After fixing α_{NN}, the CMGM calculations with the ENNA have been made to search for the parameter λ that may provide the best possible description of the elastic data. The input parameters and the χ^2/N values, obtained in this way, are collected in Table 1. Set 1 and Set 2 in this Table are the related values by using the σ^f_{NN} and the σ^m_{NN}, respectively.

The calculated elastic cross sections for α + ^{16}O system at E_{lab} = 240 and 400 MeV are presented in Fig. 1 and 2, along with the experimental data [16,17]. The upper and lower parts of Figs. 1 and 2 are the calculated results by using σ^f_{NN} and σ^m_{NN}, respectively, and corresponding input parameters are given in Set 1 and Set 2 of Table 1. The dotted and solid curves are the results by using the CNNA and the ENNA, respectively. For each calculation, we can find that the results with the σ^m_{NN} were found to do better in reproducing the experimental data than those with the σ^f_{NN}. As Table 1 shows, the χ^2/N values for each incident energy are lower in the calculated results with the σ^m_{NN} than the ones with the σ^f_{NN}. The improved agreements with the elastic data indicate that introducing the in-medium NN total cross

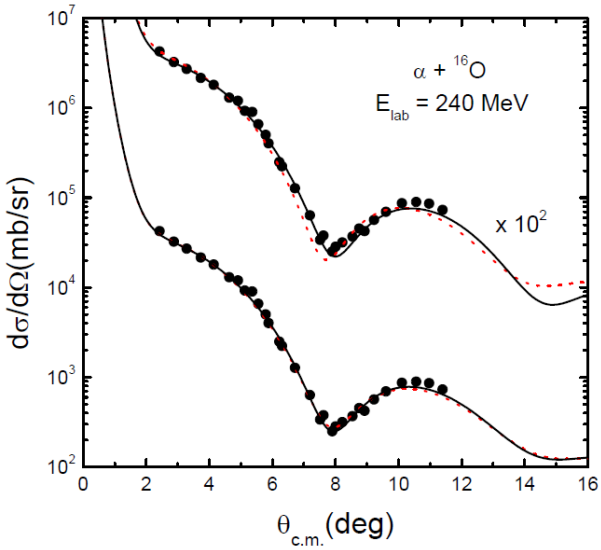

Fig. 1. (Color online) Elastic scattering angular distributions for the α + ^{16}O at E_{lab} = 240 MeV. The solid circles denote the experimental data taken from Ref. [16]. The upper and lower parts are the calculated results by using the free and in-medium NN total cross sections, respectively. The dotted and solid curves are the results by using the conventional and the effective NN amplitudes, respectively.

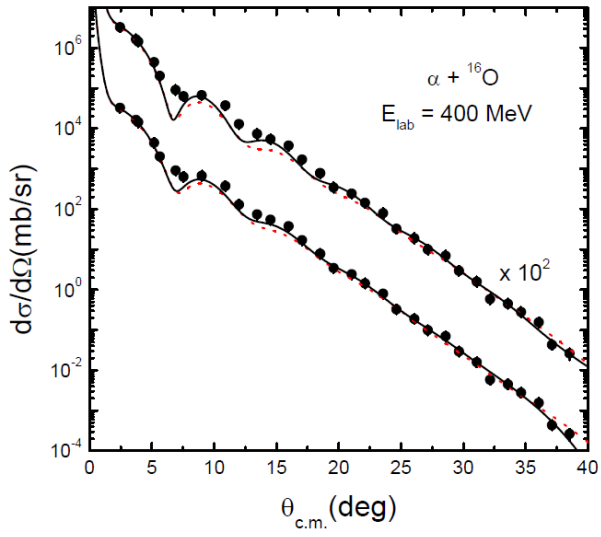

Fig. 2. (Color online) The same as Fig. 1, but for the α + ^{16}O at E_{lab} = 400 MeV. The experimental data are taken from Ref. [17].

section is important in the description of α + ^{16}O elastic scattering. Thus, we will analyze the elastic data by using the CMGM with the σ_{NN}^{m} from now on. The lower parts of Figs. 1 and 2 show the calculated results by using the CNNA (dotted curves) and ENNA (solid curves) with the σ_{NN}^{m}, respectively. As seen in these figures, the

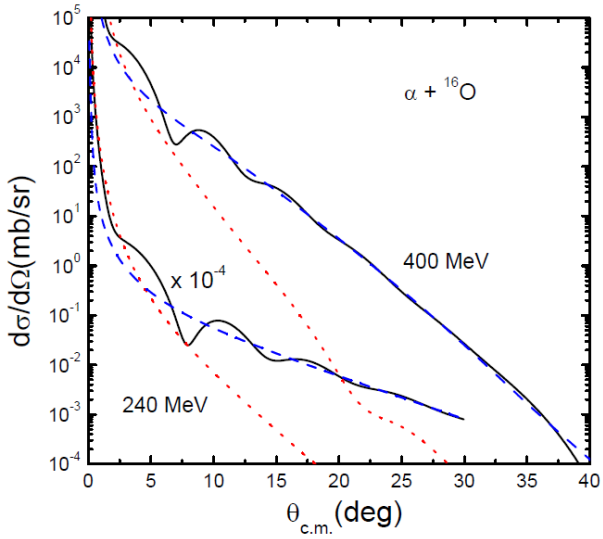

Fig. 3. (Color online) Differential cross sections (solid curves), near-side contributions (dotted curves), and far-side contributions (dashed curves) following the Fuller's formalism [22] obtained from the CMGM by using the effective NN amplitude with in-medium NN total cross section for the elastic scattering of α + ^{16}O at E_{lab} = 240 MeV and 400 MeV, respectively.

differences between the dotted and solid curves are substantial when compared to the experimental data. In particular, the solid curves reproduced well the heights and depths of maxima and minima of elastic data, in comparison with the dotted curves. In addition, the solid curve of Fig. 2 gave some difference at smooth exponential falloff regions. As these figures and Table 1 show, solid curves give lower χ^2/N values and bring the elastic cross sections closer to the experimental data compared with the dotted curves. This means that the ENNA helps in reproducing the heavy-ion elastic scattering data.

The near- and the far-side decompositions of the scattering amplitudes by using the ENNA with σ_{NN}^{m} were also performed by following the Fuller's formalism [22]. The contributions of the near-side (dotted curves) and the far-side (dashed curves) components to the cross sections are shown in Fig. 3 along with the differential cross sections (solid curves). The differential cross-section is not just a sum of the near- and the far-side cross-sections but contains the interference between the near- and the far-side amplitudes as shown in Fig. 3. The oscillations observed in the elastic scattering cross sections for α + ^{16}O system at E_{lab} = 240 and 400 MeV are due to an interference between the near- and the far-side components. As Fig. 3 and Table 2 show, the magnitudes of the

Table 2. Analysis results of the CMGM by using the effective NN amplitude with in-medium NN total cross section for the $\alpha + {}^{16}$O elastic scattering at 240 and 400 MeV.

Energy (MeV)	$\theta_{cross}(deg)$	$\theta_{n.r.}(deg)$	$L_{1/2}$	$R_s(fm)$	$\sigma_{R_s}(mb)$	$\sigma_R(mb)$
240	4.4	-45.0	26.48	5.036	797	805
400	3.3	-11.2	31.38	4.590	662	693

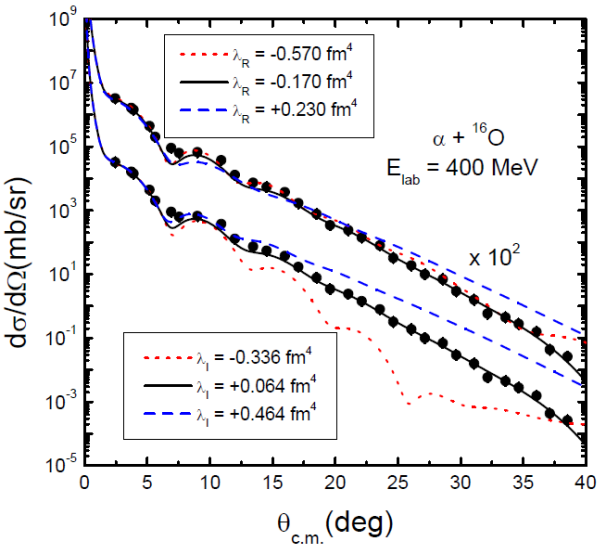

Fig. 4. (Color online) Elastic scattering angular distributions obtained from the different λ_R (upper part) and λ_I (lower part) values, corresponding to the coefficients of q^4 in the effective NN amplitude with in-medium NN total cross section, for the $\alpha + {}^{16}$O elastic scattering at $E_{lab} = 400$ MeV. The other input parameters are given as Set 2 in Table 1.

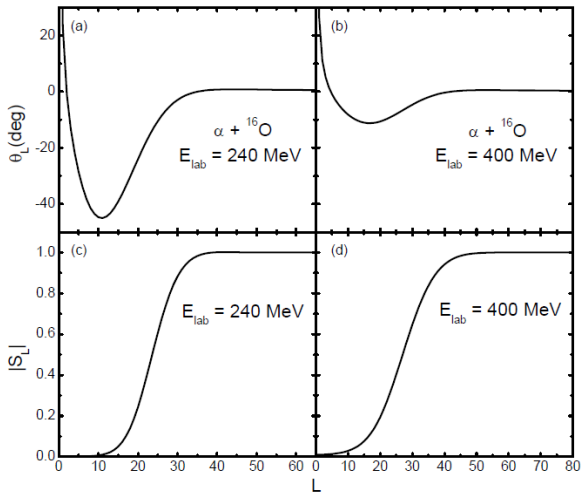

Fig. 5. (Color online) Deflection function (θ_L) and modulus of the S-matrix elements ($|S_L|$) obtained from the CMGM by using the effective NN amplitude with in-medium NN total cross section for $\alpha + {}^{16}$O elastic scattering versus the orbital angular momentum L.

near- and far-side contributions are equal, at the crossing angles $\theta_{cross} = 4.4°$ for $E_{lab} = 240$ MeV and $\theta_{cross} = 3.3°$ for at $E_{lab} = 400$ MeV. The behaviors of large-angle cross sections are mainly determined by the far-side amplitude.

To investigate the effect of a λq^4 component in ENNA on the elastic cross section, we plotted the angular distributions (using Set 2 in Table 1) of $\alpha + {}^{16}$O at $E_{lab} = 400$ MeV in terms of the real (λ_R) and imaginary (λ_I) parts of λ, where the other input parameters are fixed. The λ_R (λ_I) value was taken ± 0.4 fm^4 from the best fit λ_R (λ_I) value, and the corresponding results are displayed in Fig. 4. The solid curve shows the best fits with λ_R (λ_I) $= -0.170$ (0.064) fm^4, while the dotted and dashed curves are the results for λ_R (λ_I) ± 0.4 fm^4. We can see that the elastic cross sections around the first maxima ($\theta_{c.m.} \simeq 9°$) are moved upward as the λ_R value decreases. On the other hand, a higher λ_I value pushes the elastic cross section to the upward as a whole compared to the calculation with lower λ_I. The parameters λ_R and λ_I also affect the reaction cross section σ_R. Three λ_R values for $E_{lab} = 400$ MeV generated somewhat different σ_R values ($\sigma_R = 678$, 693 and 700 mb for $\lambda_R = -0.570$, -0.170 and 0.230 fm^4), and λ_I values produced also different values ($\sigma_R = 673$, 693 and 701 mb for $\lambda_I = -0.336$, 0.064 and 0.464 fm^4), indicating that the σ_R increases as the λ_R (or λ_I) value becomes larger. Similar results were also obtained for $E_{lab} = 240$ MeV.

The deflection functions (using Set 2 in Table 1) given by the formula, $\theta_L = 2(d/dL)(\sigma_L + \mathrm{Re}\delta_L)$, are plotted in Fig. 5 along with the corresponding modulus of $S-$matrix elements, $|S_L|$. In a nuclear rainbow situation, the strong nuclear force attracts the projectiles towards the scattering center and deflects them to negative scattering angles. The deflection functions have typical negative extreme value associated with the nuclear rainbow angle $\theta_{n.r.}$. As Table 2 and Fig. 5(a)-(b) show, the $\theta_{n.r.}$

are -45.0° for E_{lab} = 240 MeV and -11.2° for E_{lab} = 400 MeV, respectively, which evidently prove a presence of the nuclear rainbow in each incident energy. It can also noticed that the magnitude of $\theta_{n.r.}$ decreases as the incident energy increases. In Fig. 5(c)-(d), we can see that the values of $|S_L|$ approach 0 at the regions of $L \to 0$, increase rapidly as the $L-$value becomes larger, and finally reach to 1. A further investigation of the situation can be gained by looking at the strong absorption radius (R_s) and the reaction cross sections (σ_{R_s} and σ_R) given in Table 2. The R_s is determined from the formula $R_s = \{\eta + \sqrt{\eta^2 + L_{1/2}(L_{1/2}+1)}\}/k$, in which $L_{1/2}$ corresponds to $|S_L|^2 = 1/2$. From the comparisons between the geometrical ($\sigma_{R_s} = \pi R_s^2$) and the partial wave sum (σ_R) reaction cross sections given in Table 2, we can find that R_s provides a good estimate of the reaction cross section.

IV. CONCLUDING REMARKS

In this paper, we have presented a Coulomb-modified Glauber model by using the effective NN amplitude considering a q^4 component. It has been applied to the $\alpha + {}^{16}$O elastic scattering at E_{lab} = 240 and 400 MeV. The CMGM by using the CNNA was first employed to determine the parameter α_{NN} from fitting the elastic data. After fixing α_{NN}, the CMGM calculations by using the ENNA were performed to search for the parameter λ by using the least-square fits. The calculated results reproduced well the structures of angular distributions and showed fairly good agreements with the experimental data for $\alpha + {}^{16}$O elastic scattering at E_{lab} = 240 and 400 MeV. Comparing to the calculated results by using σ_{NN}^f, the differential cross sections with the σ_{NN}^m gave improved agreements with the experimental data. Regardless of using the σ_{NN}^f or the σ_{NN}^m, the results by using the ENNA provided better agreements with the experimental data, especially at the maximum region and the large angles, in comparison with the ones by using CNNA. This implies that CMGM including the q^4 component in NN amplitude with in-medium NN total cross section helps in reproducing the $\alpha + {}^{16}$O elastic scattering data.

Through the near-side and the far-side decompositions of elastic cross section, we have also shown that the oscillatory structure observed in the angular distributions is considered to be due to the interference between the near-side and the far-side amplitudes. The behaviors of the large-angle cross sections are mainly determined by the far-side amplitude. The presence of a nuclear rainbow in both incident energy is evidenced through a classical deflection function. The magnitude of the maximum negative deflection angle for E_{lab} = 240 MeV is larger than the one for E_{lab} = 400 MeV, indicating that the nuclear rainbow angle value decreases as the incident energy increases. We can see that the higher momentum transfer component ($(\lambda_R + i\lambda_I)q^4$) in ENNA has a influence on the elastic and reaction cross sections. When other input parameters are fixed, a higher λ_I value moved the elastic cross section to the upward as a whole, in comparison with the calculation with lower λ_I. The reaction cross section has been found to increase as the λ_R (or λ_I) value increases.

ACKNOWLEDGEMENTS

This work was supported by the Project-"PoINT" of Jeju National University in 2016.

REFERENCES

[1] V. Franco and A. Tekou, Phys. Rev. C **16**, 658 (1977).
[2] J. Chauvin, D. Lebrun, A. Lounis and M. Buenerd, Phys. Rev. C **28**, 1970 (1983).
[3] A. Vitturi and F. Zardi, Phys. Rev. C **36**, 1404 (1987).
[4] S. K. Charagi and S. K. Gupta, Phys. Rev. C **41**, 1610 (1990).
[5] S. K. Charagi and S. K. Gupta, Phys. Rev. C **46**, 1982 (1992).
[6] S. K. Charagi and S. K. Gupta, Phys. Rev. C **56**, 1171 (1997).
[7] P. Shukla, Phys. Rec. C **67**, 054607 (2003).
[8] M. A. Alvi, M. R. Arafah and F. S. Al-Hazmi, J. Phys. G: Nucl. Part. Phys. **37**, 045101 (2010).

[9] A. A. Ibraheem, Int. J. Mod. Phys. E **20**, 721 (2011).
[10] M. A. M. Hassan, M. S. M. Nour El-Din, A. Ellithi, E. Ismail and H. Hosny, Int. J. Mod. Phys. E **24**, 1550062 (2015).
[11] S. K. Charagi, Phys. Rev. C **48**, 452 (1993).
[12] M. A. Alvi, J. H. Madani and A. M. Hakmi, Phys. Rev. C **75**, 064609 (2007).
[13] D. Chauhan and Z. A. Khan, Eur. Phys. J. A **41**, 179 (2009).
[14] M. H. Cha and Y. J. Kim, J. Phys. G: Nucl. Part. Phys. **17**, L95 (1991).
[15] Y. J. Kim, New Phys.: Sae Mulli **66**, 151 (2016).
[16] Y. W. Lui, H. L. Clark and D. H. Youngblood, Phys. Rev. C **64**, 064308 (2001).
[17] T. Wakasa, E. Ihara, K. Fujita, Y. Funaki and K. Hatanaka *et al.*, Phys. Lett. B **653**, 173 (2007).
[18] I. Ahmad, M. A. Abdulmomen and M. A. Alvi, Int. J. Mod. Phys. E **11**, 519 (2002).
[19] I. Ahmad and M. A. Alvi, Int. J. Mod. Phys. E **13**, 1225 (2004).
[20] C. Xiangzhou, F. Jun, S. Wenqing, M. Yugang and W. Jiansong *et al.*, Phys. Rev. C **58**, 572 (1998).
[21] M. M. H. El-Gogary, A. S. Shalaby, M. Y. Hassan and A. M. Hegazy, Phys. Rev. C **61**, 044604 (2000).
[22] R. C. Fuller, Phys. Rev. C **12**, 1561 (1975).